

Article

HIV Dynamics with a Trilinear Antibody Growth Function and Saturated Infection Rate

Fatima Ezzahra Fikri * and Karam Allali * 

Laboratory of Mathematics Computer Science and Applications, Faculty of Sciences and Technologies,
University Hassan II of Casablanca, Mohammedia P.O. Box 146, Morocco

* Correspondence: fikri.uh2c@gmail.com (F.E.F.); allali@hotmail.com (K.A.)

Abstract: The objective of this paper is to study a new mathematical model describing the human immunodeficiency virus (HIV). The model incorporates the impacts of cytotoxic T lymphocyte (CTL) immunity and antibodies with trilinear growth functions. The boundedness and positivity of solutions for non-negative initial data are proved, which is consistent with biological studies. The local stability of the equilibrium is established. Finally, numerical simulations are presented to support our theoretical findings.

Keywords: antibody response; CTL response; HIV infection; numerical simulation; viral dynamics



Citation: Fikri, F.E.; Allali, K. HIV Dynamics with a Trilinear Antibody Growth Function and Saturated Infection Rate. *Math. Comput. Appl.* **2022**, *27*, 85. <https://doi.org/10.3390/mca27050085>

Academic Editors: Stephen Moore, Emmanuel K. Essel and Osei K. Tweneboah

Received: 3 September 2022

Accepted: 3 October 2022

Published: 8 October 2022

Publisher's Note: MDPI stays neutral with regard to jurisdictional claims in published maps and institutional affiliations.



Copyright: © 2022 by the authors. Licensee MDPI, Basel, Switzerland. This article is an open access article distributed under the terms and conditions of the Creative Commons Attribution (CC BY) license (<https://creativecommons.org/licenses/by/4.0/>).

1. Introduction

The human immunodeficiency virus (HIV) is a virus that causes, at the end stage of infection, acquired immunodeficiency syndrome (AIDS). The human system then fails to perform its functions [1,2]. Several mathematical models of HIV dynamics have been developed in recent decades [3–7]. For example, reference [8] investigates a model representing the interaction between $CD4^+$ T cells, HIV contagions, and cytotoxic T lymphocyte (CTL) growth using two saturated rates defining viral infection and CTL proliferation. The authors demonstrate how the cellular immune response may be used to restrict the spread of HIV infections. Several recent studies have emphasized the importance of antibodies in reducing viral replication and improving patient quality of life [9–12]. The relevance of antibodies in infection control was recently examined by the authors of [13]. The essential novelty here is that antibody growth is dependent not only on the virus and antibody concentrations, but also on the uninfected cells' concentration. It is very important, since the role of the immune response to HIV infection has been recently recognized by the medical literature to be of great value. Indeed, it is now well known that the CTL immune response increases depending on the infection. This increase also depends on the number of CTLs themselves. Moreover, the antibody immune response increases depending on the virus proliferation, and this growth also depends on the number of viruses. As the growth of the immune system cells depends on the number of healthy target cells ($CD4^+$ T cells), the development of immune responses is described using a trilinear term [14–16]. The objective of the HIV virus is to destroy $CD4^+$ T cells, often called messengers or the command centers of the immune system. Once the virus invades the body, these cells send a message to the immune system. CTLs and antibodies represent the immune system, which responds to this message and sets out to eliminate the infection by killing infected cells and free viruses. To include the antibodies in the model, their participation in controlling the infection is thus essential. Additionally, a comparison between simulations with HIV ordinary differential equation models and clinical data has been done in [17,18]. The following model has been presented:

$$\begin{cases} \frac{dx}{dt} = \lambda - dx - \beta xv, \\ \frac{dy}{dt} = \beta xv - ay - pyz, \\ \frac{dv}{dt} = aNy - \mu v - qvw, \\ \frac{dz}{dt} = cxyz - hz, \\ \frac{dw}{dt} = gxvw - \sigma w \end{cases}$$

In this model, $x(t), y(t), v(t), z(t)$, and $w(t)$, denote the concentrations of uninfected cells, infected cells, HIV virus, CTLs, and antibodies, respectively, at time t . The healthy $CD4^+$ T cells (x) grow at a rate λ , die at a rate d , and become infected by the virus at a rate βxv . Infected cells (y), die at a rate a and are killed by the CTLs response at a rate p . Free virus (v) is produced by the infected cells at a rate aN , die at a rate μ , and decay in the presence of antibodies at a rate q , where N is the number of free viruses produced by each actively infected cell during its life time. CTLs (z) expand in response to viral antigen derived from infected cells at a rate c and decay in the absence of antigenic stimulation at a rate h . Finally, antibodies (w) develop in response to free viruses at a rate g and decay at a rate σ . It is worthwhile to note that all the model rates are assumed to be non-negative. We are interested in the same topic in this study, but we include the function of the CTL immune response and saturation rate in the model. The nonlinear system of five differential equations under investigation is as follows:

$$\begin{cases} \frac{dx}{dt} = \lambda - dx - \frac{\beta xv}{1 + \alpha v}, \\ \frac{dy}{dt} = \frac{\beta xv}{1 + \alpha v} - ay - pyz, \\ \frac{dv}{dt} = aNy - \mu v - qvw, \\ \frac{dz}{dt} = cxyz - hz, \\ \frac{dw}{dt} = gxvw - \sigma w \end{cases} \tag{1}$$

where α is the saturated infection rate and the initial conditions are $x(0) = x_0, y(0) = y_0, v(0) = v_0, z(0) = z_0$, and $w(0) = w_0$.

The paper is organized as follows. Section 2 is devoted to the existence, positivity, and boundedness of solutions. The analysis of the model is carried out in Section 3. Then, in Section 4, the results are illustrated through numerical simulations. We finish in Section 5 with our conclusions.

2. Positivity and Boundedness of Solutions

It is generally known that any solutions reflecting cell densities should be non-negative and bounded. Therefore, it will be useful to establish the positivity and boundedness of solutions of the model (1). First of all, for biological results, the initial data x_0, y_0, v_0, z_0 , and w_0 must be larger than or equal to 0. The main result of this section is given as follows:

Proposition 1. *For any non-negative initial conditions, the solutions to the problem (1) exist. In addition, this solution is non-negative and bounded for all $t \geq 0$.*

Proof. First, we show that the non-negative $\mathbb{R}_+^5 = \{(x, y, v, z, w) \in \mathbb{R}^5 : x \geq 0, y \geq 0, v \geq 0, z \geq 0 \text{ and } w \geq 0\}$ is positively invariant. Additionally, for $(x(t), y(t), v(t), z(t), w(t)) \in \mathbb{R}_+^5$, we have:

$$\begin{aligned} \dot{x}_{x=0} = \lambda \geq 0, \quad \dot{y}_{y=0} = \frac{\beta xv}{1 + \alpha v} \geq 0, \quad \dot{v}_{v=0} = aNy \geq 0, \\ \dot{z}_{z=0} = 0 \geq 0, \quad \text{and} \quad \dot{w}_{w=0} = 0 \geq 0. \end{aligned}$$

Therefore, all solutions initiating in \mathbb{R}_+^5 are positive. Next, we prove that these solutions remain bounded. By adding the two first equations in (1), we have $\dot{B} = \lambda - dx - ay - pyz$; thus,

$$B(t) \leq B(0)e^{-\delta t} + \frac{\lambda}{\delta} (1 - e^{-\delta t}),$$

where $B(t) = x(t) + y(t)$ and $\delta = \min(a; d)$. Since $1 - e^{-\delta t} \leq 1$ and $0 \leq e^{-\delta t} \leq 1$, we deduce that $B(t) \leq B(0) + \frac{\lambda}{\delta}$. Therefore, x and y are bounded. From the equation $\dot{v} = aNy - \mu v - qvw$, we deduce that

$$v(t) \leq v(0)e^{-\mu t} + aN \int_0^t y(\xi)e^{(\xi-t)\mu} d\xi.$$

Then,

$$v(t) \leq v(0) + \frac{aN}{\mu} \|y\|_{\infty} (1 - e^{-\mu t}).$$

Since $1 - e^{-\mu t} \leq 1$, we have $v(t) \leq v(0) + \frac{aN}{\mu} \|y\|_{\infty}$. Thus, v is bounded. Now, we prove the boundedness of z . From the fourth equation of (1), we have

$$\dot{z}(t) + hz(t) = cx(t)y(t)z(t).$$

Moreover, from the second equation of (1), it follows that

$$\dot{z}(t) + hz(t) = \frac{c}{p} x(t)(\beta x(t)v(t) - ay(t) - \dot{y}(t)).$$

By integrating over time, we have

$$z(t) = z(0)e^{-ht} + \int_0^t \frac{c}{p} x(s)(\beta x(s)v(s) - ay(s) - \dot{y}(s))e^{h(s-t)} ds.$$

From the boundedness of x, y , and v , and by using integration by parts, the boundedness of z follows. The two equations $\dot{v}(t) = aNy(t) - \mu v(t) - qv(t)w(t)$ and $\dot{w}(t) = gx(t)v(t)w(t) - \sigma w(t)$ imply

$$\dot{w}(t) + \sigma w(t) = gx(t)v(t)w(t) = \frac{g}{q} x(t)(aNy(t) - \dot{v}(t) - \mu v(t)).$$

Then,

$$w(t) = w(0)e^{-\sigma t} + \int_0^t \frac{g}{q} x(s)(aNy(s) - \mu v(s) - \dot{v}(s))e^{\sigma(s-t)} ds.$$

From the boundedness of x, y , and v , the boundedness of w follows. \square

We established the well-posedness of the proposed model in this research, ensuring that all solutions exist and are bounded. This is consistent with the biological fact that these populations' overall cell numbers are limited.

3. Analysis of the Model

In this section, we determine the steady states of the model (1).

3.1. Stability of the Disease-Free Equilibrium

The basic reproductive number of the system (1), is given by

$$R_0 = \frac{\beta\lambda N}{d\mu}.$$

From a biological point of view, R_0 denotes the average number of secondary infections generated by one infected cell when all cells are uninfected. Moreover, the same system has the following disease-free equilibrium:

$$E_f = \left(\frac{\lambda}{d}, 0, 0, 0, 0 \right).$$

At any arbitrary point, the Jacobian matrix of the system (1) is given by

$$J = \begin{pmatrix} -d - \frac{\beta v}{1+\alpha v} & 0 & \frac{-\beta x}{(1+\alpha v)^2} & 0 & 0 \\ \frac{\beta v}{1+\alpha v} & -a - pz & \frac{\beta x}{(1+\alpha v)^2} & -py & 0 \\ 0 & aN & -\mu - qw & 0 & -qv \\ cyz & cxz & 0 & cxy - h & 0 \\ gv w & 0 & gxw & 0 & gxv - \sigma \end{pmatrix}.$$

Proposition 2. The disease-free equilibrium, E_f , is locally asymptotically stable for $R_0 < 1$.

Proof. At the disease-free equilibrium, E_f , the Jacobian matrix is given as follows:

$$J_{E_f} = \begin{pmatrix} -d & 0 & -\frac{\beta\lambda}{d} & 0 & 0 \\ 0 & -a & \frac{\beta\lambda}{d} & 0 & 0 \\ 0 & aN & -\mu & 0 & 0 \\ 0 & 0 & 0 & -h & 0 \\ 0 & 0 & 0 & 0 & -\sigma \end{pmatrix}.$$

The characteristic polynomial of J_{E_f} is

$$P_{E_f}(X) = a_0X^5 + a_1X^4 + a_2X^3 + a_3X^2 + a_4X^1 + a_5,$$

where

$$a_0 = 1,$$

$$a_1 = \sigma + h + \mu + a + d,$$

$$a_2 = \frac{\sigma da + ad^2 + hda + \mu da + \sigma d^2 + \sigma dh + \sigma d\mu + hd^2 + \mu d^2 + hd\mu - aN\beta\lambda}{d},$$

$$a_3 = \frac{a\sigma d^2 + a\sigma dh + a\sigma d\mu + ad^2h + \mu d^2a + adh\mu + \sigma d^2h + \sigma d^2\mu + \sigma dh\mu + d^2h\mu - \frac{aN\sigma\beta\lambda + \alpha N\beta\lambda d + aNh\beta\lambda}{d}}{d},$$

$$a_4 = \frac{a\sigma d^2h + a\sigma d^2\mu + a\sigma dh\mu + ad^2h\mu + \sigma d^2h\mu - aN\sigma d\beta\lambda - aN\sigma h\beta\lambda - aNd h\beta\lambda}{d},$$

$$a_5 = \sigma h\mu da(1 - R_0).$$

By the Routh–Hurwitz theorem [19] applied to the fifth-order polynomial, the eigenvalues of the Jacobian matrix have negative real parts, since we have $a_1 > 0$, $a_1a_2 > a_3$, $a_1a_2a_3 > a_1^2a_4$, and $a_1a_2a_3a_4 > a_1a_2^2a_5 + a_1^2a_4^2$. Consequently, we obtain the asymptotic local stability of the disease-free equilibrium E_f . □

3.2. Infection Steady States

We now show the existence and stability of the infected steady states. All these steady states exist when the basic reproduction number exceeds unity, and disease invasion is always possible. In fact, it is easily verified that the system (1) has four of them:

$$\begin{aligned}
 E_1 &= (x_1, y_1, v_1, 0, 0), \\
 x_1 &= \frac{\mu(dR_0 + \lambda)}{N\lambda(\alpha d + \beta)}, \quad y_1 = \frac{d\mu(R_0 - 1)}{aN(\alpha d + \beta)}, \quad v_1 = \frac{d\mu(R_0 - 1)}{\mu(\alpha d + \beta)}. \\
 E_2 &= (x_2, y_2, v_2, z_2, 0), \\
 x_2 &= \frac{\lambda(\alpha v_2 + 1)}{\alpha d v_2 + \beta v_2 + d}, \quad y_2 = \frac{\mu}{aN} v_2, \\
 z_2 &= \frac{a(-\alpha d \mu v_2 + N\beta\lambda - d\mu - \beta\mu v_2)}{p\mu(\alpha d v_2 + \beta v_2 + d)}, \\
 v_2 &= \frac{\sqrt{a^2 h^2 (\alpha d + \beta)^2 N^2 + 2a\chi u \lambda (\alpha d - \beta) N + c^2 \lambda^2 u^2} + (\alpha d + \beta) h a N - c \lambda u}{2\alpha c \lambda u}. \\
 E_3 &= (x_3, y_3, v_3, 0, w_3), \\
 x_3 &= \frac{\lambda(\alpha v_3 + 1)}{\alpha d v_3 + \beta v_3 + d}, \quad y_3 = \frac{\beta\lambda}{a(\alpha d v_3 + \beta v_3 + d)} v_3, \\
 w_3 &= \frac{-\alpha d \mu v_3 + N\beta\lambda - \beta\mu v_3 - d\mu}{q(\alpha d v_3 + \beta v_3 + d)}, \\
 v_3 &= \frac{(\alpha d + \beta)\sigma - g\lambda + \sqrt{(\alpha d + \beta)^2 \sigma^2 + 2g\lambda(\alpha d - \beta)\sigma + g^2 \lambda^2}}{2g\lambda\alpha}. \\
 E_4 &= (x_4, y_4, v_4, z_4, w_4), \\
 x_4 &= \frac{\lambda(\alpha v_4 + 1)}{\alpha d v_4 + \beta v_4 + d}, \quad y_4 = \frac{gh}{\sigma c} v_4, \quad w_4 = \frac{Nagh - \sigma c \mu}{\sigma c q}, \\
 z_4 &= -\frac{a\alpha d g h v_4 + a\beta g h v_4 + a d g h - \alpha \beta c \lambda}{g p h (\alpha d v_4 + \beta v_4 + d)}, \\
 v_4 &= \frac{(\alpha d + \beta)\sigma - g\lambda + \sqrt{(\alpha d + \beta)^2 \sigma^2 + 2g\lambda(\alpha d - \beta)\sigma + g^2 \lambda^2}}{2g\lambda\alpha}.
 \end{aligned}$$

In this case, the endemic equilibrium point E_1 represents the equilibrium case in the absence of an adaptive immune response. The endemic equilibrium points E_2 and E_3 define the equilibrium case in the presence of only one kind each of adaptive immune response, antibody response, and CTL response, respectively. The last endemic equilibrium point, E_4 , is for chronic HIV infection with the presence of both kinds of adaptive immune response, CTLs and antibody. To study the stability of the points E_1, E_2, E_3 , and E_4 , we need the following reproduction numbers:

$$\begin{aligned}
 R_1 &= \frac{u(\alpha d + \beta)}{(N\alpha\lambda + u)\beta}, \\
 R_2 &= \frac{N(N\alpha\beta g \lambda^2 - \alpha^2 d^2 \sigma - \alpha d g \lambda u - 2\alpha\beta d \sigma + \beta g \lambda u - \beta^2 \sigma)}{u^2 d g}, \\
 R_3 &= \frac{g}{2c\sigma\mu} \frac{\left(aNh(\alpha d + \beta) + \sqrt{aN^2h^2(\alpha d + \beta)^2 + 2aNch\lambda\mu(\alpha d - \beta) + c^2\lambda^2\mu^2} \right)^2 - c^2\lambda^2\mu^2}{\left((\alpha d + \beta) \left(aNh(\alpha d + \beta) - c\lambda\mu + \sqrt{aN^2h^2(\alpha d + \beta)^2 + 2aNch\lambda\mu(\alpha d - \beta) + c^2\lambda^2\mu^2} \right) + 2d\alpha c\lambda\mu \right)},
 \end{aligned}$$

and

$$R_4 = \frac{c\beta\lambda^2\alpha}{ah} \frac{\left(\sigma(\alpha d + \beta) + \sqrt{\sigma^2(\alpha d + \beta)^2 + 2\sigma g(\alpha d - \beta) + g^2\lambda^2 + g\lambda}\right)}{\left((\alpha d + \beta)\left(\sigma(\alpha d + \beta) + \sqrt{\sigma^2(\alpha d + \beta)^2 + 2\sigma g(\alpha d - \beta) + g^2\lambda^2}\right) + g\lambda(\alpha d - \beta)\right)}.$$

For the first point, E_1 , we have the following result.

Proposition 3. *If $R_0 > 1$, then E_1 is locally asymptotically stable for $R_2 < 1$ and $R_1 < 1$.*

Proof. If $R_0 > 1$, then the Jacobian matrix at E_1 is given by

$$J_{E_1} = \begin{pmatrix} -d - \beta \frac{v_1}{1+\alpha v_1} & 0 & -\beta \frac{x_1}{(1+\alpha v_1)^2} & 0 & 0 \\ \beta \frac{v_1}{1+\alpha v_1} & -a & \beta \frac{x_1}{(1+\alpha v_1)^2} & -py_1 & 0 \\ 0 & aN & -\mu & 0 & -qv_1 \\ 0 & 0 & 0 & cx_1y_1 - h & 0 \\ 0 & 0 & 0 & 0 & gx_1v_1 - \alpha \end{pmatrix}.$$

Its characteristic equation is

$$(cx_1y_1 - h - X)(gx_1v_1 - \sigma - X)(b_0X^3 + b_1X^2 + b_2X + b_3) = 0$$

where

$$\begin{aligned} b_0 &= 1, \\ b_1 &= a + d + \mu + \frac{\beta d(R_0 - 1)}{\beta + \alpha d R_0}, \\ b_2 &= a\mu + d(a + \mu) + \frac{1}{\beta + \alpha d R_0}(\beta d(a + \mu)(R_0 - 1) - a\mu d(\beta + \alpha d)), \\ b_3 &= a\mu d + \frac{\beta(a\mu d(R_0 - 1) - a\lambda N d(\beta + \alpha d)\left(R_0 - 1 - \frac{1}{R_0}\left(1 - \frac{\lambda\alpha}{d} - \frac{\mu}{dN}\right)\right))}{\beta + \alpha d R_0}. \end{aligned}$$

Direct calculations lead to

$$gx_1v_1 - \sigma = A_1(R_2 - 1) \text{ and } cx_1y_1 - h = B_1(R_1 - 1)$$

with

$$A_1 = \frac{dg\mu}{N(\alpha d + \beta)^2} \text{ and } B_1 = \frac{dc\mu^2}{aN^2(\alpha d + \beta)^2}$$

The sign of the eigenvalue $A_1(R_2 - 1)$ is negative if $R_2 < 1$, zero if $R_2 = 1$, and positive if $R_2 > 1$. The sign of the eigenvalue $B_1(R_1 - 1)$ is negative if $R_1 < 1$, zero if $R_1 = 1$, and positive if $R_1 > 1$. On the other hand, we have $b_1 > 0$ and $b_1 - b_2b_3 > 0$ (as $R_0 > 1$). From the Routh–Hurwitz theorem [19], the other eigenvalues of the above matrix have negative real parts. □

For the second endemic-equilibrium point E_2 , we have the following result.

Proposition 4. *If $R_1 > 1$ and $R_3 \leq 1$, then E_2 is locally asymptotically stable.*

Proof. We assume that $R_1 > 1$. The Jacobian matrix of E_2 is given as follows:

$$J_{E_2} = \begin{pmatrix} -d - \frac{\beta v_2}{1 + \alpha v_2} & 0 & -\frac{\beta x_2}{(1 + \alpha v_2)^2} & 0 & 0 \\ \frac{\beta v_2}{1 + \alpha v_2} & -a - pz_2 & \frac{\beta x_2}{(1 + \alpha v_2)^2} & -py_2 & 0 \\ 0 & aN & -\mu & 0 & -qv_2 \\ cy_2z_2 & cx_2z_2 & 0 & cx_2y_2 - h & 0 \\ 0 & 0 & 0 & 0 & gx_2v_2 - \sigma \end{pmatrix}$$

The characteristic equation of the system (1) at the point E_2 is given by

$$(gx_2v_2 - \sigma - X)(c_0X^4 + c_1X^3 + c_2X^2 + c_3X + c_4) = 0$$

where

$$c_0 = 1,$$

$$c_1 = d + a + \mu + \frac{\beta v_2}{1 + \alpha v_2} + pz_2,$$

$$c_2 = \left(d + \frac{\beta v_2}{1 + \alpha v_2}\right)(a + \mu) + a\mu + pz_2\left(d + \mu + h + \frac{\beta v_2}{1 + \alpha v_2}\right) - \frac{aN\beta x_2}{(1 + \alpha v_2)^2},$$

$$c_3 = a\mu\left(d + \frac{\beta v_2}{1 + \alpha v_2}\right) + pz_2\left(\mu d + hd + \mu h + \mu\frac{\beta v_2}{1 + \alpha v_2} + h\frac{\beta v_2}{1 + \alpha v_2}\right) - \frac{aN\beta dx_2}{(1 + \alpha v_2)^2},$$

$$c_4 = pz_2\left(\mu hd + \mu h\frac{\beta v_2}{1 + \alpha v_2} - aN\beta hy_2\right).$$

Simple calculations lead to

$$gx_2v_2 - \sigma = \sigma(R_3 - 1).$$

Then, $gx_2v_2 - \sigma = \sigma(R_3 - 1)$ is an eigenvalue of J_{E_2} . The sign of this eigenvalue is negative if $R_3 < 1$, null when $R_3 = 1$, and positive if $R_3 > 1$. On the other hand, from the Routh–Hurwitz theorem [19], the other eigenvalues of the above matrix have negative real parts when $R_1 > 1$. □

For the third endemic-equilibrium point E_3 , the following result holds.

Proposition 5. *If $R_2 > 1$, then E_3 is locally asymptotically stable for $R_4 < 1$.*

Proof. We assume that $R_2 > 1$. The Jacobian matrix of the system at point E_3 is given by

$$J_{E_3} = \begin{pmatrix} -d - \frac{\beta v_3}{1 + \alpha v_3} & 0 & -\frac{\beta x_3}{(1 + \alpha v_3)^2} & 0 & 0 \\ \beta\frac{\beta v_3}{1 + \alpha v_3} & -a & \frac{\beta x_3}{(1 + \alpha v_3)^2} & -py_3 & 0 \\ 0 & aN & -\mu - qw_3 & 0 & -qv_3 \\ 0 & 0 & 0 & cx_3y_3 - h & 0 \\ gv_3w_3 & 0 & gx_3w_3 & 0 & gx_3v_3 - \sigma \end{pmatrix}.$$

The characteristic equation associated with J_{E_3} is given by

$$(cx_3y_3 - h - X)(d_0X^4 + d_1X^3 + d_2X^2 + d_3X + d_4) = 0$$

where

$$\begin{aligned}
 d_0 &= 1, \\
 d_1 &= a + d + \mu + \frac{\beta v_3}{1 + \alpha v_3} + qw_3, \\
 d_2 &= \left(d + \frac{\beta v_3}{1 + \alpha v_3}\right)(a + \mu) + a\mu + \left(d + a + \sigma + \frac{\beta v_3}{1 + \alpha v_3}\right)qw_3 - aN\frac{\beta x_3}{(1 + \alpha v_3)^2}, \\
 d_3 &= a\mu\left(d + \frac{\beta v_3}{1 + \alpha v_3}\right) + \left(ad + \sigma d + a\sigma + a\frac{\beta v_3}{1 + \alpha v_3}\right)qw_3 - aNd\frac{\beta x_3}{(1 + \alpha v_3)^2}, \\
 d_4 &= ad\sigma qw_3.
 \end{aligned}$$

Here, $cx_3y_3 - h$ is an eigenvalue of J_{E_3} . By assuming $cx_3y_3 - h = h(R_4 - 1)$, we deduce that the sign of this eigenvalue is negative when $R_4 < 1$, zero when $R_4 = 1$, and positive for $R_4 > 1$. On the other hand, from the Routh–Hurwitz theorem [19], the other eigenvalues of the above matrix have negative real parts when $R^W > 1$. Consequently, E_3 is locally asymptotically stable when $R_2 > 1$ and $R_4 < 1$. □

For the last endemic-equilibrium point E_4 , we prove the following result.

Proposition 6. *If $R_3 > 1$ and $R_4 > 1$, then E_4 is locally asymptotically stable.*

Proof. The Jacobian matrix of the system at the point E_4 is given by

$$J_{E_4} = \begin{pmatrix} -d - \frac{\beta v_4}{1 + \alpha v_4} & 0 & -\frac{\beta x_4}{(1 + \alpha v_4)^2} & 0 & 0 \\ \frac{\beta v_4}{1 + \alpha v_4} & -a - pz_4 & \frac{\beta x_4}{(1 + \alpha v_4)^2} & -py_4 & 0 \\ 0 & aN & -\mu - qw_4 & 0 & -qv_4 \\ cy_4z_4 & cx_4z_4 & 0 & cx_4y_4 - h & 0 \\ gv_4w_4 & 0 & gx_4w_4 & 0 & gx_4v_4 - \sigma \end{pmatrix}$$

The characteristic equation associated with J_{E_4} is given by

$$f_0X^5 + f_1X^4 + f_2X^3 + f_3X^2 + f_4X + f_5 = 0$$

where

$$\begin{aligned}
 f_0 &= 1, \\
 f_1 &= a + d + \mu + \frac{\beta v_4}{1 + \alpha v_4} + pz_4 + qw_4, \\
 f_2 &= \left(d + \frac{\beta v_4}{1 + \alpha v_4}\right)(a + \mu) + a\mu + pz_4\left(d + h + \mu + \frac{\beta v_4}{1 + \alpha v_4} + qw_4\right) \\
 &\quad + qw_4\left(d + a + \sigma + \frac{\beta v_4}{1 + \alpha v_4}\right) - aN\frac{\beta x_4}{(1 + \alpha v_4)^2}, \\
 f_3 &= a\mu\left(d + \frac{\beta v_4}{1 + \alpha v_4}\right) + pz_4\left(d\mu + dh + \mu h + \mu\frac{\beta v_4}{1 + \alpha v_4} + h\frac{\beta v_4}{1 + \alpha v_4}\right) \\
 &\quad + qw_4\left(ad + \sigma d + a\sigma + a\frac{\beta v_4}{1 + \alpha v_4}\right) + pqz_4w_4\left(d + \sigma + h + \frac{\beta v_4}{1 + \alpha v_4}\right) \\
 &\quad - aNd\frac{\beta x_4}{(1 + \alpha v_4)^2}, \\
 f_4 &= adqw_4 + pz_4\left(dh\mu + \mu h\frac{\beta v_4}{1 + \alpha v_4} - aN\beta hy_4\right) + pqz_4w_4\left(d\sigma + \sigma\frac{\beta v_4}{1 + \alpha v_4} + h\sigma\right), \\
 f_5 &= \sigma hd\left(pqz_4w_4 + aN\frac{\beta v_4}{1 + \alpha v_4}\left(1 - \frac{\beta x_4}{1 + \alpha v_4}\right)\right).
 \end{aligned}$$

From the Routh–Hurwitz theorem applied to the five-order polynomial, the eigenvalues of the Jacobian matrix have negative real parts, since we have $f_1 > 0$, $f_1 f_2 > f_3$, $f_1 f_2 f_3 > f_1^2 f_4$, and $f_1 f_2 f_3 f_4 > f_1 f_2^2 f_5 + f_1^2 f_4^2$. Consequently, we can obtain the asymptotic local stability of the endemic point E_4 . \square

4. Numerical Simulations

The numerical simulations were performed using in-house code run in MATLAB software. To solve numerically the five differential equations of the system (1), numerical simulations have been carried out. The simulation parameters were derived from [13,19–21]. Our first numerical simulations were focused on demonstrating the importance of antibodies to reducing infection severity. Other numerical simulations was used to verify our theoretical findings. We also take into account the initial conditions given as follows: $x_0 = 5, y_0 = 1, v_0 = 1, z_0 = 1$, and $w_0 = 1$.

Figure 1 shows the development of the infection in the free equilibrium case: $d = 0.007$, $\beta = 0.00025$, $a = 0.2$, $p = 1$, $\mu = 2.06$, $c = 0.0051$, $h = 0.004$, $\lambda = 1$, $N = 6.25$, $g = 0.00013$, $q = 0.12$, $\alpha = 10^{-4}$, and $\sigma = 0.12$. Within these chosen parameters, we have the basic reproduction number being less than unity $R_0 = 0.1084 < 1$, and we can observe the convergence of the curves corresponding to the stability of the disease-free equilibrium $E_f = (142.8571, 0, 0, 0, 0)$. This confirms our theoretical result given in Proposition 2.

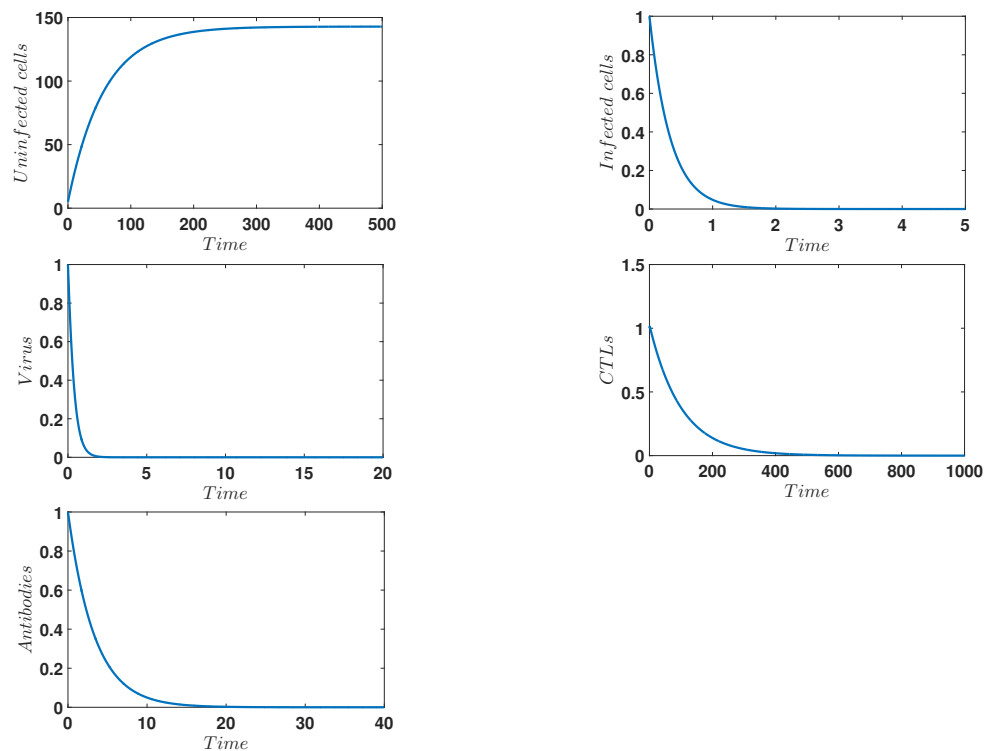


Figure 1. Behavior of the infection over time for $d = 0.007$, $\beta = 0.00025$, $a = 0.2$, $p = 1$, $\mu = 2.06$, $c = 0.0051$, $h = 0.004$, $\lambda = 1$, $N = 6.25$, $g = 0.00013$, $q = 0.12$, $\alpha = 10^{-4}$, and $\sigma = 0.12$, which corresponds to the stability of the free equilibrium $E_f = (142.8571, 0, 0, 0, 0)$ with ($R_0 = 0.1084 < 1$).

Figure 2 shows the infection dynamics for the following parameters: $d = 0.1$, $\beta = 0.000024$, $a = 0.002$, $\mu = 3$, $c = 5.8 \times 10^{-6}$, $h = 0.23$, $\lambda = 10$, $N = 2640$, $g = 1.3 \times 10^{-6}$, $q = 5 \times 10^{-9}$, $\alpha = 10^{-5}$, and $\sigma = 0.2$. With these parameters we can easily compute the reproduction numbers $R_0 = 2.1120 > 1$ and $R_1 = 0.7535 < 1$, which means that the first one is greater than unity, and the second is less than one. This predicts numerical stability of the first endemic equilibrium, E_1 . Indeed, we can observe that the curves converge toward the first endemic equilibrium $E_1 = (85.8342, 479.1444, 800.2941, 0, 0)$, which confirms our theoretical finding concerning the stability of E_1 .

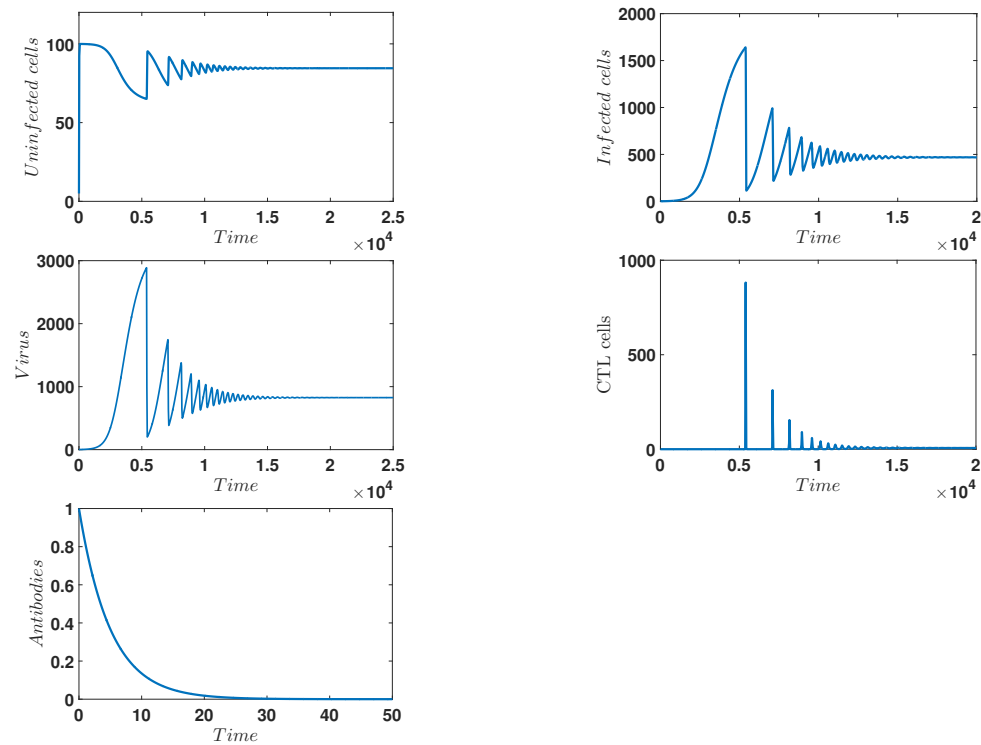


Figure 2. Behavior of the infection in time for $d = 0.1$, $\beta = 0.000024$, $a = 0.002$, $\mu = 3$, $c = 5.8 \times 10^{-6}$, $h = 0.23$, $\lambda = 10$, $N = 2640$, $g = 1.3 \times 10^{-6}$, $q = 5 \times 10^{-9}$, $\alpha = 10^{-5}$, and $\sigma = 0.2$, which corresponds to the stability of the endemic equilibrium point $E_1 = (85.8342, 479.1444, 800.2941, 0, 0)$ with $(R_0 = 2.1120 > 1$ and $R_1 = 0.7535 < 1)$.

Figure 3 shows the infection dynamics for the following parameters: $d = 0.05$, $\beta = 0.000024$, $a = 0.0017$, $p = 0.0001$, $\mu = 2.06$, $c = 3.9 \times 10^{-6}$, $h = 0.15$, $\lambda = 12$, $N = 2640$, $g = 1.3 \times 10^{-6}$, $q = 5 \times 10^{-9}$, $\alpha = 10^{-11}$, and $\sigma = 20$. With these parameters we can easily compute the reproduction numbers $R_1 = 1.0010 > 1$ and $R_3 = 0.0325 < 1$. This predicts the numerical stability of the second endemic equilibrium, E_2 . Indeed, we can observe that the curves converge toward the second endemic equilibrium $E_2 = (199.7789, 192.5205, 419.4330, 87.4592, 0)$, which confirms our theoretical finding concerning the stability of E_2 . Additionally, Figure 4 shows the infection dynamics for the following parameters: $d = 0.05$, $\beta = 0.000024$, $a = 0.001$, $p = 0.0001$, $\mu = 2.06$, $c = 2.4 \times 10^{-6}$, $h = 0.26$, $\lambda = 14$, $N = 2640$, $g = 1.3 \times 10^{-6}$, $q = 5 \times 10^{-9}$, $\alpha = 10^{-11}$, and $\sigma = 0.1$. With these parameters, we can easily compute the reproduction numbers $R_2 = 3.6200 > 1$ and $R_4 = 0.1318 < 1$. This predicts the numerical stability of the third endemic equilibrium, E_3 . Indeed, we observe that the curves converge toward the third endemic equilibrium, $E_3 = (246.9057, 434.8010, 279.2416, 0, 4.168 \times 10^8)$, which confirms our theoretical finding concerning the stability of E_3 . Figures 3 and 4 show the actions of the disease in the absence of CTLs and antibody responses, respectively.

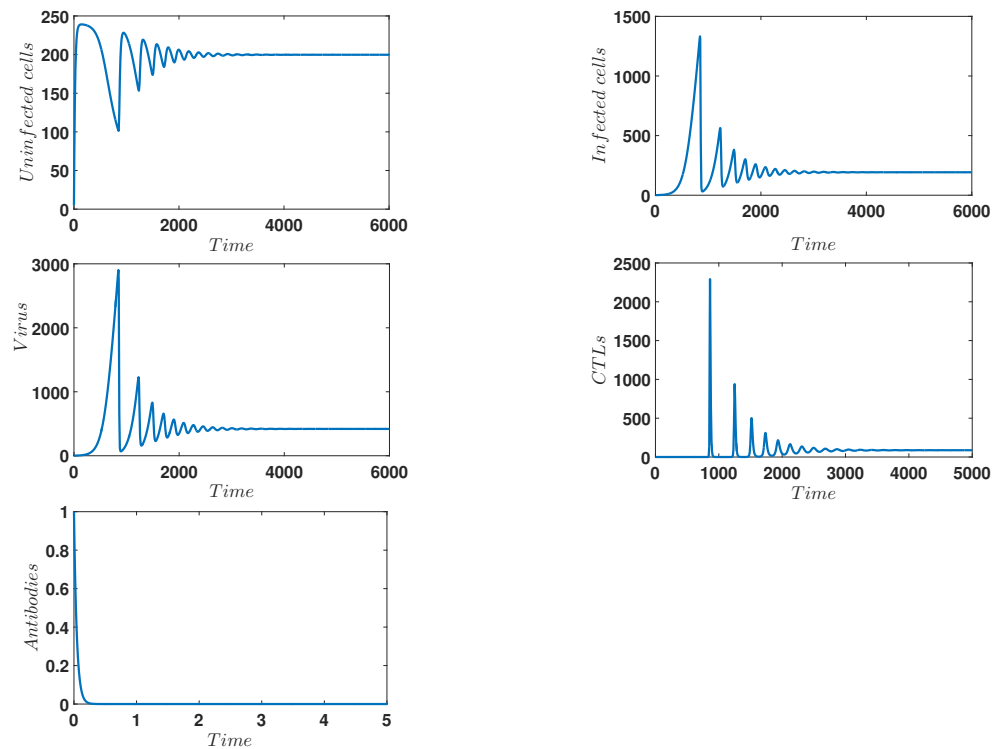


Figure 3. Behavior of the infection over time for $d = 0.05$, $\beta = 0.000024$, $a = 0.0017$, $p = 0.0001$, $\mu = 2.06$, $c = 3.9 \times 10^{-6}$, $h = 0.15$, $\lambda = 12$, $N = 2640$, $g = 1.3 \times 10^{-6}$, $q = 5 \times 10^{-9}$, $\alpha = 10^{-11}$, and $\sigma = 20$, which corresponds to the stability of the endemic equilibrium $E_2 = (199.7789, 192.5205, 419.4330, 87.4592, 0)$ with $(R_1 = 1.0010 > 1$ and $R_3 = 0.0325 < 1)$.

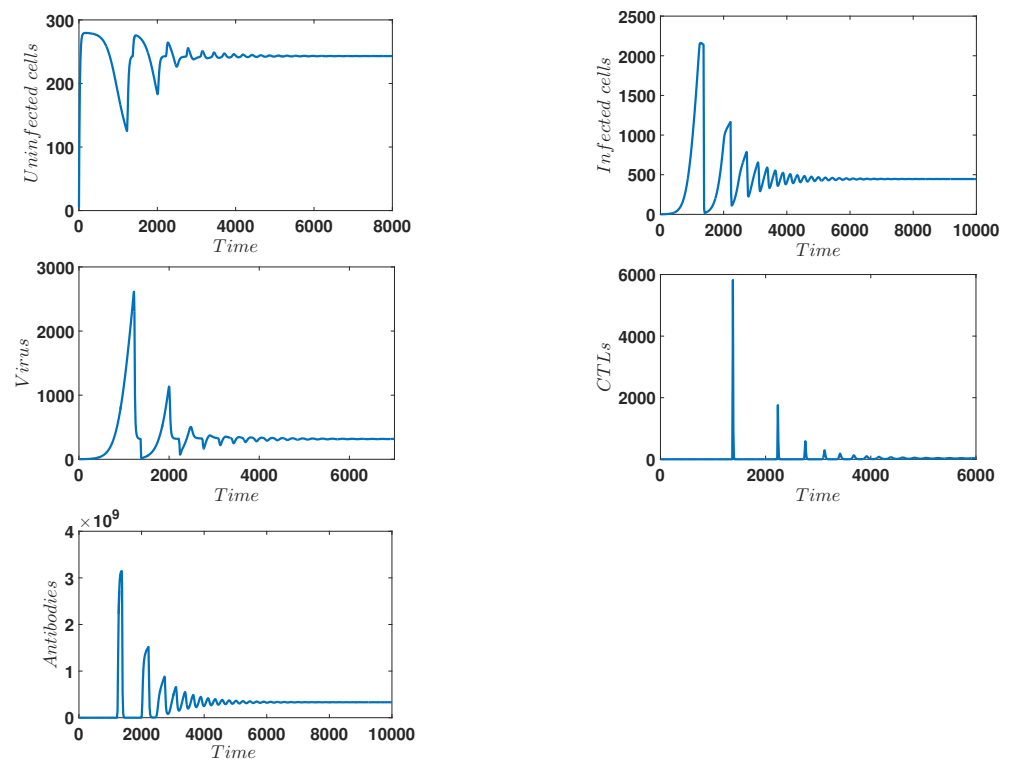


Figure 4. Behavior of the infection over time for $d = 0.05$, $\beta = 0.000024$, $a = 0.001$, $p = 0.0001$, $\mu = 2.06$, $c = 2.4 \times 10^{-6}$, $h = 0.26$, $\lambda = 14$, $N = 2640$, $g = 1.3 \times 10^{-6}$, $q = 5 \times 10^{-9}$, $\alpha = 10^{-11}$, and $\sigma = 0.1$, which corresponds to the stability of the endemic equilibrium $E_3 = (246.9057, 434.8010, 279.2416, 0, 4.168 \times 10^8)$ with $(R_2 = 3.6200 > 1$ and $R_4 = 0.1318 < 1)$.

Finally, Figure 5 shows the infection dynamics for the following parameters: $d = 0.05$, $\beta = 0.000024$, $a = 0.0017$, $p = 0.0001$, $\mu = 2.06$, $c = 3.9 \times 10^{-6}$, $h = 0.15$, $\lambda = 12$, $N = 2640$, $g = 1.3 \times 10^{-6}$, $q = 5 \times 10^{-9}$, $\alpha = 10^{-11}$, and $\sigma = 0.1$. With these parameters we can easily compute the reproduction numbers $R_3 = 1.0200 > 1$ and $R_4 = 2.4652 > 1$; both of them are greater than unity. This predicts the numerical stability of the fourth endemic equilibrium, E_4 . Indeed, we can observe that the curves converge toward the fourth endemic equilibrium $E_4 = (208.5510, 1982.7148, 420.251, 104.9445, 3.6800 \times 10^7)$, which confirms our theoretical finding concerning the stability of E_4 of model (1), which is globally asymptotically stable; this is consistent with Proposition 6. Figure 5 shows the actions of the complaint in the presence of all the variables acting on the model. The figure shows the continuity of HIV contagion. Additionally, we observe that the two immunity systems may control the infection better than only one immunity type. We have observed many oscillations like those in many previous works in the literature [22,23]. We have studied numerically the stability of the problem's equilibria. We have found that the numerical tests are consistent with the theoretical results.

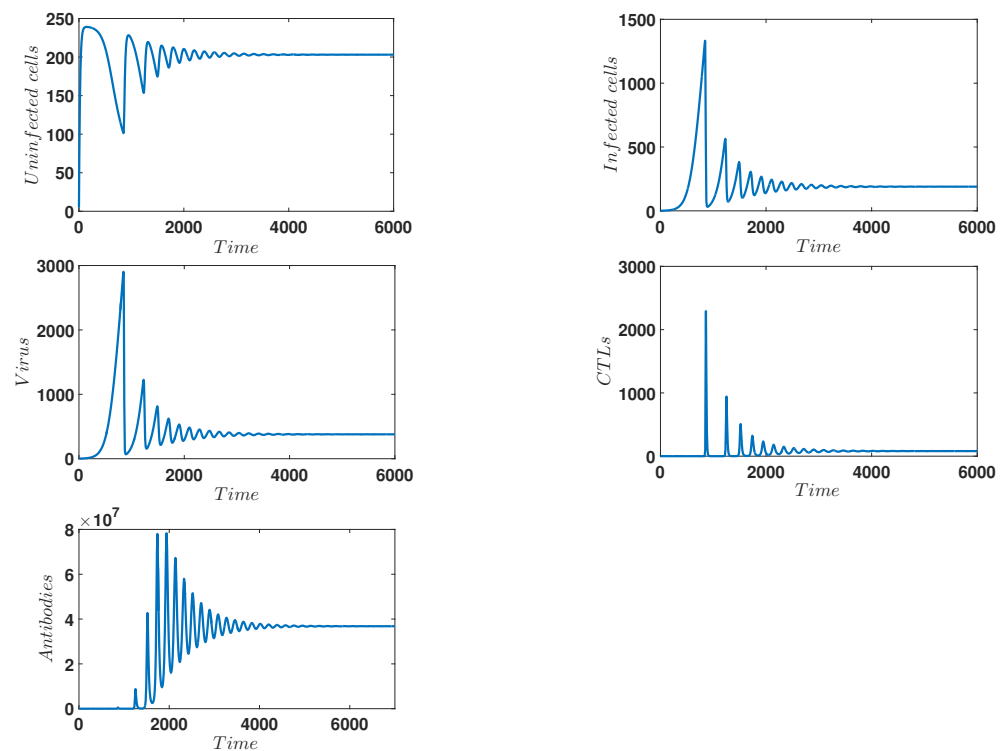


Figure 5. Behavior of the infection over time for $d = 0.05$, $\beta = 0.000024$, $a = 0.0017$, $p = 0.0001$, $\mu = 2.06$, $c = 3.9 \times 10^{-6}$, $h = 0.15$, $\lambda = 12$, $N = 2640$, $g = 1.3 \times 10^{-6}$, $q = 5 \times 10^{-9}$, $\alpha = 10^{-11}$, and $\sigma = 0.1$, which corresponds to the stability of the endemic equilibrium $E_4 = (208.5510, 1982.7148, 420.251, 104.9445, 3.6800 \times 10^7)$ with ($R_3 = 1.0200 > 1$ and $R_4 = 2.4652 > 1$).

5. Conclusions

In this paper, we presented and investigated a new mathematical model of human immunodeficiency illness by considering the adaptive immune response and a trilinear antibody growth function. The model's primary innovation is that it considers how antibody formation is influenced not only by illness and antibody concentration, but also by the concentration of uninfected cells, which has been validated by current findings. The boundedness and positivity of the findings were established once the new mathematical model was proposed. The local stability of the disease-free and infection-stable states was also investigated. Other numerical simulations were also carried out in order to verify the theoretical conclusions on equilibrium stability.

Author Contributions: F.E.F.: Conceptualization, Validation, Formal analysis, Software, Writing—review and editing; K.A.: Conceptualization, Validation, Formal analysis, Writing—review, editing and Supervision. All authors have read and agreed to the published version of the manuscript.

Funding: This research received no external funding.

Conflicts of Interest: The authors declare no conflict of interest.

References

1. Weiss, R. How does HIV cause AIDS? *Science* **1993**, *260*, 1273–1279 [[CrossRef](#)]
2. Blanttner, W.; Gallo, R.; Temin, H. HIV causes aids. *Science* **1988**, *241*, 515–516. [[CrossRef](#)]
3. Bairagi, N.; Adak, D. Global analysis of HIV-1 dynamics with Hill type infection rate and intracellular delay. *Appl. Math. Model.* **2014**, *38*, 5047–5066. [[CrossRef](#)]
4. Balasubramaniam, P.; Prakash, M.; Rihan, F.A.; Lakshmanan, S. Hopf bifurcation and stability of periodic solutions for delay differential model of HIV infection of CD4⁺ T-cells. *Abstr. Appl. Anal.* **2014**, *2014*, 838396. [[CrossRef](#)]
5. Rihan, F.A.; Rahman, D.H.A. Delay differential model for tumour–immune dynamics with HIV infection of CD4⁺ T-cells. *Int. J. Comput. Math.* **2013**, *90*, 594–614. [[CrossRef](#)]
6. Nowak, M.; May, R. Mathematical biology of HIV infection: Antigenic variation and diversity threshold. *Math. Biosci.* **1991**, *106*, 1–21. [[CrossRef](#)]
7. Perelson, A.; Nelson, P. Mathematical analysis of HIV-1 dynamics in vivo. *SIAM Rev.* **1999**, *41*, 3–44. [[CrossRef](#)]
8. Tabit, Y.; Hattaf, K.; Yousfi, N. Dynamics of an HIV pathogenesis model with CTL immune response and two saturated rates. *World J. Model. Simul.* **2014**, *10*, 215–223.
9. Chun, T.W.; Murray, D.; Justement, J.S.; Blazkova, J.; Hallahan, C.W.; Fankuchen, O.; Gittens, K.; Benko, E.; Kovacs, C.; Moir, S.; et al. Broadly neutralizing antibodies suppress HIV in the persistent viral reservoir. *Proc. Natl. Acad. Sci. USA* **2014**, *111*, 13151–13156. [[CrossRef](#)] [[PubMed](#)]
10. Geib, Y.; Dietrich, U. The race between HIV and neutralizing antibodies. *AIDS Rev.* **2015**, *17*, 107–113.
11. West, A.P., Jr.; Scharf, L.; Scheid, J.F.; Klein, F.; Bjorkman, P.J.; Nussenzweig, M.C. Structural insights on the role of antibodies in HIV-1 vaccine and therapy. *Cell* **2014**, *156*, 633–648. [[CrossRef](#)] [[PubMed](#)]
12. Zhou, Y.; Yang, K.; Zhou, K.; Wang, C. Optimal Treatment Strategies for HIV with Antibody Response. *J. Appl. Math.* **2014**, *2014*, 685289. [[CrossRef](#)]
13. Allali, K.; Harroudi, S.; Torres, D.F.M. Optimal control of HIV model with a trilinear antibody growth function. *arXiv* **2021**, arXiv:2105.10291.
14. Wodarz, D. Helper-dependent vs. helper-independent CTL responses in HIV infection: Implications for drug therapy and resistance. *J. Theor. Biol.* **2001**, *213*, 447–459. [[CrossRef](#)] [[PubMed](#)]
15. Wang, Y.; Zhou, Y.; Brauer, F.; Heffernan, J.M. Viral dynamics model with CTL immune response incorporating antiretroviral therapy. *J. Math. Biol.* **2013**, *67*, 901–934. [[CrossRef](#)]
16. Zhu, H.; Zou, X. Dynamics of a HIV-1 infection model with cell-mediated immune response and intracellular delay. *Discrete Contin. Dyn. Syst. Ser. B* **2009**, *12*, 511–524. [[CrossRef](#)]
17. Stafford, M.A.; Corey, L.; Cao, Y.; Daar, E.S.; Ho, D.D.; Perelson, A.S. Modeling plasma virus concentration during primary HIV infection. *J. Theor. Biol.* **2000**, *203*, 285–301. [[CrossRef](#)]
18. Danane, J.; Allali, K. Mathematical analysis and clinical implications of an HIV Model with adaptive immunity. *Comput. Math. Methods Med.* **2019**, *2019*, 7673212. [[CrossRef](#)]
19. Gradshteyn, I.S.; Ryzhik, I.M. Table of integrals, series, and products. *Math. Comput.* **1982**, *39*, 747–757.
20. van den Driessche, P. Reproduction numbers of infectious disease models. *Infect. Dis. Model.* **2017**, *2*, 288–303. [[CrossRef](#)]
21. Tabit, Y.; Meskaf, A.; Allali, K. Mathematical analysis of HIV model with two saturated rates, CTL and antibody responses. *World J. Model. Simul.* **2016**, *12*, 137–146.
22. Lim, S.C.; Eab, C.H.; Mak, K.H.; Li, M.; Chen, S.Y. Solving linear coupled fractional differential equations by direct operational method and some applications. *Math. Probl. Eng.* **2012**, *2012*, 653939. [[CrossRef](#)]
23. Kartal, S.; Gurcan, F. Discretization of conformable fractional differential equations by a piecewise constant approximation. *Int. J. Comput. Math.* **2019**, *96*, 1849–1860. [[CrossRef](#)]